JOURNAL OF SOLID STATE CHEMISTRY **129,** 320–327 (1997)
ARTICLE NO. SC967259

A Study of the Structure and Electronic and Thermal Properties of Quasi-One-Dimensional La_3MoO_7

J. E. Greedan[1], N. P. Raju, and A. Wegner

Brockhouse Institute for Materials Research and Department of Chemistry, McMaster University, Hamilton, Canada L8S 4M1

and

P. Gougeon and J. Padiou

Laboratoire du Chimie du Solide et Inorganique Moleculaire, U.R.A. 1495, Universite de Rennes I, Avenue du General Leclerc, 35042 Rennes Cedex, France

Received September 30, 1996; in revised form December 2, 1996; accepted December 5, 1996

The structure of La_3MoO_7 was solved in $P2_12_12_1$ with $Z = 4$ and $a = 7.597(1)$ Å, $b = 7.7192(4)$ Å, and $c = 11.0953(8)$ Å and refined to the reliability factors of $R(F) = 0.0366$ and $wR(F2) = 0.0782$ for 102 variables and 5352 reflections. A structural feature of interest is the presence of zigzag chains of *trans*-corner-sharing octahedra of composition MoO_5^{5-} parallel to the *b*-axis. Resistivity data taken along the *b*-axis direction show semiconducting behavior in the range 140 to 298 K with an activation energy of 0.16 eV. The magnetic susceptibility is quite complex. The main feature is a broad maximum at 655 K which is interpreted as due to intrachain spin correlations of the Mo(5 +) ions. Assuming the $S = 1/2$ Heisenberg model this implies a $J/k = -511$ K. Several other anomalies are observed at 483, 140, and 100 K. Differential scanning calorimetry data also show the 483 K feature and disclose another at 373 K not seen in the susceptibility. There is no evidence from powder neutron diffraction data of any structural changes from 298 to 10 K but no data are available above room temperature. There is an indication from neutron diffraction data for the onset of long-range antiferromagnetic order below 100 K.

INTRODUCTION

Compounds of the composition Ln_3MO_7, where M is a pentavalent 4*d* or 5*d* transition element such as Nb, Mo, Ru, Ir, or Ta or even the main group element Sb and Ln is a rare earth crystal in an ordered fluorite structure with orthorhombic symmetry (1–9). Various space groups have been suggested including *Pnma*, *Cmcm*, and $C222_1$, although the correct space group is unknown in several cases, especially M = Mo.

All descriptions of this particular type of ordered fluorite structure feature zigzag chains of *trans*-corner-shared octahedra of composition MO_5^{5-} which are parallel to one of the orthorhombic axes and are well separated by seven or eightfold coordinate Ln–O polyhedra.

The presence of the MO_5^{5-} chains suggests that the electronic properties of these compounds, especially electrical transport and magnetism, should reflect this low-dimensional feature. There have been relatively few studies of any electronic properties for this class of compounds. The magnetic susceptibility of Pr_3MO_7 phases where M is diamagnetic, M = Nb, Ta, or Sb, represents an exception (7). Also, susceptibility data for an impure sample of La_3MoO_7 have been reported (4).

In this study we have reinvestigated La_3MoO_7 as it represents one of the most interesting cases with a $4d^1$ ion on the M sites and diamagnetic La^{3+} on the Ln sites. The possibilities are especially rich for d^1 systems and include Peierls or spin–Peierls distortions, short-range linear chain magnetism, and long-range magnetic order due to interchain coupling. Single crystal and polycrystalline samples have been prepared using high temperature methods. The crystal structure has been refined from single crystal X-ray data at room temperature and powder neutron data at lower temperatures. Resistivity data have been obtained on single crystals and magnetic susceptibility studies have been performed on powder samples over a wide temperature range. Low temperature neutron diffraction data have been examined for the presence of long-range magnetic order.

EXPERIMENTAL

Preparation of Polycrystalline La_3MoO_7

The polycrystalline sample of La_3MoO_7 used for the susceptibility and neutron diffraction studies was prepared

[1] To whom correspondence should be addressed.

0022-4596/97 $25.00

by reaction of a well-ground mixture of La_2O_3, MoO_2, and MoO_3 in a welded molybdenum crucible under an argon atmosphere at 1300°C for 30 h. La_2O_3 was prefired at 1000°C. Successful preparations were also achieved by reduction of $La_6Mo_2O_{15}$ at 1250°C in a $CO/CO_2 = 1$ buffer gas mixture for 3 h. $La_6Mo_2O_{15}$ was prepared from a mixture of La_2O_3 and excess MoO_3 (to allow for volatility) at 1400°C in air for 72 h. Phase purity was checked by powder X-ray diffraction and unit cell constants were refined from data obtained using a Guinier–Hagg camera and Cu$K\alpha_1$ radiation with a Si internal standard. The Guinier films were read with a computer controlled LS-20 line scanner (KEJ Instruments, Taby, Sweden)

The refined unit cell constants were $a = 7.5985(5)$ Å, $b = 7.7201(5)$ Å, $c = 11.1014(6)$ Å, and $V = 651.2$ Å^3 for the welded tube preparation which compares well with the cell derived from the single crystal X-ray study.

Crystal Growth

Starting reagents were La_2O_3 (Rhône-Poulenc, 99.999%), MoO_3 (Strem Chemicals, 99.9%), and Mo, all in powder form. The rare earth sesquioxide was prefired at 1000°C before use and the Mo powder was heated under a hydrogen flow at 1000°C for 6 h. The mixture in molar ratio 6:5:7 was pressed into pellets and loaded into a molybdenum crucible which was sealed under a low argon pressure using an arc welding system. Single crystals could be obtained by heating the charge at the rate 300°C/h to 1700°C which was held for 48 h. The charge was then cooled at 100°C/h down to 1100°C and finally furnace cooled.

X-Ray Diffraction

A needle-like crystal of the approximate dimensions $0.5 \times 0.045 \times 0.022$ mm was selected for data collection. Intensity data were collected by the 2θ scan method on a CAD4 Enraf-Nonius diffractometer using graphite-monochromatized Mo$K\alpha$ radiation ($\lambda = 0.71073$ Å) at room temperature. The intensities of three standard reflections showed no significant variations over the data collection. The data set was corrected for Lorentz and polarization effects and for absorption by employing a ψ-scan method (10) on six reflections. Analysis of the data revealed that the systematic absences ($h00$) $h = 2n + 1$, ($0k0$) $k = 2n + 1$, and ($00l$) $l = 2n + 1$ were consistent only with the acentric orthorhombic space group $P2_12_12_1$. The lattice constants were determined by least squares refinement of the setting angles of 25 reflections in the 2θ range 10°–34° that had been automatically centered on the diffractometer. Starting positions for La, Mo, and O in the present study were derived from the atomic coordinates of La, Nb, and O in La_3NbO_7 which crystallizes in the *Pnma* space group (8), a super group of $P2_12_12_1$. Full-matrix least-squares refinement on F^2 on all positional and anisotropic thermal parameters including terms for anisotropic extinction was employed. An attempt to establish the absolute configuration was made by refining Flack's x parameter (11). The resulting value of 0.48 (4) gave evidence that the crystal studied is a racemic twin. The final refinement which was based on a model with two components of racemic twinnning led to the values of $R(F) = 0.0366$ and $wR(F2) = 0.0782$ for all data and a twinning parameter of 0.56 (11). The final electron density map shows no peaks of height greater than 2.3% that of a La atom. Because the U_{11} term of La(1) was larger than those of La(2) and La(3), a model where the La(1) position was split into two positions with an occupancy of 50% was considered. Refinements on this model were unsuccessful. On the other hand, it should be noted that the equivalent La atom in La_3NbO_7 behaves similarly. Refinements of the occupancy factors for the four cationic sites yield values of 0.996 (2), 0.998 (2), 1.000 (2), and 1.000 (2) for Mo, La(1), La(2), and La(3), respectively, and show that they are fully occupied. Calculations were performed on a Digital Pentium Celebris 590 FP for SHELXL-93 (12) and on a Digital micro VAX 3100 for the MOLEN (13) program (data reduction and absorption corrections). The crystallographic and experimental data are summarized in Table 1. The final atomic coordinates and temperature factors are reported in Table 2 and selected interatomic distances and angles in Table 3.

Magnetic Susceptibility

Magnetic measurements were made over the range 5–800 K using a MPMS SQUID magnetometer (Quantum Design). The region from 300 to 800 K was accessible by means of an oven insert.

Neutron Diffraction

Neutron diffraction data were obtained on the DUALSPEC high resolution powder diffractometer at the Chalk River Nuclear Laboratories of AECL. The powder sample was placed in a vanadium can and sealed with an indium gasket under a helium atmosphere. Neutron wavelengths of 2.314 and 2.367 Å were used on different occasions and the sample was cooled in a liquid helium cryostat. Temperatures were controlled to $+/-0.1$ K.

Resistivity Measurement

The dc resistivity measurement was made on a single crystal parallel to the *b*-axis with a current of 5 nA using a standard four-probe technique between 300 and 77 K. Ohmic contacts were made by attaching molten indium ultrasonically.

TABLE 1
Crystallographic and Experimental Data for La_3MoO_7

Formula	La_3MoO_7
Molecular weight	2498.68
Crystal system	Orthorhombic
Space group	$P2_12_12_1$
a(Å)	7.597(1)
b(Å)	7.7192(4)
c(Å)	11.0953(8)
V(Å)^3	650.6(2)
Density (calc., g·cm^{-3})	6.375
Temperature (K)	293
Diffractometer	Enraf-Nonius CAD4
Radiation	Mo$K\alpha$ radiation ($\lambda = 0.71073$ Å)
Crystal color	Black
Morphology	needle
Crystal size (mm^3)	$0.5 \times 0.045 \times 0.022$
Linear absorption coeff. (mm^{-1})	21.160
Monochromator	Oriented graphite
Scan mode	θ–2θ
Recording range $2\theta^\circ$	2–90
hkl range	0/15, 0/15, −22/22
No. of measured reflections	5854
No. of independent reflections	5352
R_{int}	0.016
Absorption correction	ψ-scan
Transmission (min. − max.)	0.606–1.000
Refinement	$F2$
Calculated weights	$w = 1/[\sigma^2(F_o2) + (0.0401P)\ 2 + 3.3186P]$, where $P = (F_o2 + 2F_c2)/3$
Extinction coefficient	0.0060(2)
$R[F > 2(F)]$	0.0298
$R(F)$ on all data	0.0366
$wR(F2)$ on all data	0.0782
S (all data)	1.112
No. of refined parameters	102

TABLE 2
Fractional Atomic Coordinates and Equivalent Isotropic Displacement Parameters (Å) La_3MoO_7

Atom	x	y	z	U_{eq}[a]
Mo	0.49769(3)	0.00092(4)	0.74965(4)	0.00439(4)
La(1)	0.98034(3)	0.00599(2)	0.75292(3)	0.00919(4)
La(2)	0.69733(2)	0.75379(3)	0.53503(2)	0.00595(4)
La(3)	0.68892(2)	0.74755(3)	−0.02027(2)	0.00597(4)
O(1)	0.5690(4)	0.7470(3)	0.7589(2)	0.0083(3)
O(2)	0.7923(5)	0.9634(4)	0.1295(3)	0.0101(5)
O(3)	0.1397(6)	0.0504(4)	0.1155(3)	0.0147(6)
O(4)	0.8288(5)	0.9627(4)	0.3729(3)	0.0101(5)
O(5)	0.1981(5)	0.0316(4)	0.3689(3)	0.0107(5)
O(6)	0.9588(4)	0.7484(5)	−0.1191(2)	0.0075(3)
O(7)	0.9874(4)	0.7568(5)	0.6182(3)	0.0080(4)

[a] $U_{eq} = 1/3\sum_i\sum_j U_{ij}a_i^*a_j^*a_ia_j$.

Differential Scanning Calorimetry

Data were obtained using a TA Instruments DSC 2910 Differential Scanning Calorimeter over the temperature range 298 to 610 K at a heating rate of 5 K/min in an argon atmosphere.

RESULTS AND DISCUSSION

Crystal Structure at $T = 298$ K

The crystal structure of La_3MoO_7 is basically similar to that of the Nb analogue, the structure of which was first determined from X-ray powder diffraction by Rossel (1979) (3) and more recently on a single crystal by Kahn-Harari *et al.* (1995) (8). It consists of slabs, parallel to the (a, b) plane, in which rows of corner-linked MoO_6 octahedra running parallel to the b-axis alternate with rows of edge-shared La(1)O8 pseudo-cubes (Figs. 1 and 2). These slabs are separated by La(2) and La(3) cations which both are seven coordinated by oxygen atoms. The MoO_6 octahedra are rather distorted as reflected by the Mo–O distances which range between 1.861 (3) and 2.098 (4) Å and by the O–Mo–O bond angles which deviate from 90° by up to 5°. The Mo–O(1)–Mo bond angle between two corner-linked octahedra is 149.1 (2)° indicating weak Mo–O–Mo interactions along the b-axis. The average Mo–O bond distance is 1.981 Å and is slightly smaller than the distance expected from the sum of the ionic radii of O^{2-} and Mo^{5+} (2.01 Å) according to Shannon and Prewitt (14). However, a similar value of 1.965 Å is observed in La_2LiMoO_6 (15) which also

TABLE 3
Selected Bond Distances (Å) and Angles (°) for La_3MoO_7

Mo–O(3)	1.861(3)	La(1)–O(7)	2.419(3)
Mo–O(4)	1.920(4)	La(1)–O(6)	2.433(3)
Mo–O(1)	1.968(2)	La(1)–O(7)	2.436(3)
Mo–O(5)	2.006(4)	La(1)–O(6)	2.449(3)
Mo–O(1)	2.036(2)	La(1)–O(2)	2.494(4)
Mo–O(2)	2.098(4)	La(1)–O(4)	2.710(4)
O(3)–Mo–O(4)	170.4(2)	La(1)–O(5)	2.776(4)
O(3)–Mo–O(1)	91.29(13)	La(2)–O(7)	2.333(3)
O(4)–Mo–O(1)	94.01(12)	La(2)–O(7)	2.389(3)
O(3)–Mo–O(5)	94.9(2)	La(2)–O(2)	2.423(3)
O(4)–Mo–O(5)	93.3(2)	La(2)–O(5)	2.448(3)
O(1)–Mo–O(5)	87.81(12)	La(2)–O(3)	2.605(3)
O(3)–Mo–O(1)	89.12(13)	La(2)–O(4)	2.614(3)
O(4)–Mo–O(1)	85.54(12)	La(2)–O(1)	2.669(3)
O(1)–Mo–O(1)	179.47(4)	La(3)–O(6)	2.325(3)
O(5)–Mo–O(1)	92.49(12)	La(3)–O(6)	2.335(3)
O(3)–Mo–O(2)	86.9(2)	La(3)–O(2)	2.481(3)
O(4)–Mo–O(2)	84.91(15)	La(3)–O(5)	2.517(3)
O(1)–Mo–O(2)	92.20(12)	La(3)–O(4)	2.535(3)
O(5)–Mo–O(2)	178.2(2)	La(3)–O(3)	2.558(3)
O(1)–Mo–O(2)	87.48(11)	La(3)–O(1)	2.614(3)
Mo–O(1)–Mo	148.6(11)		

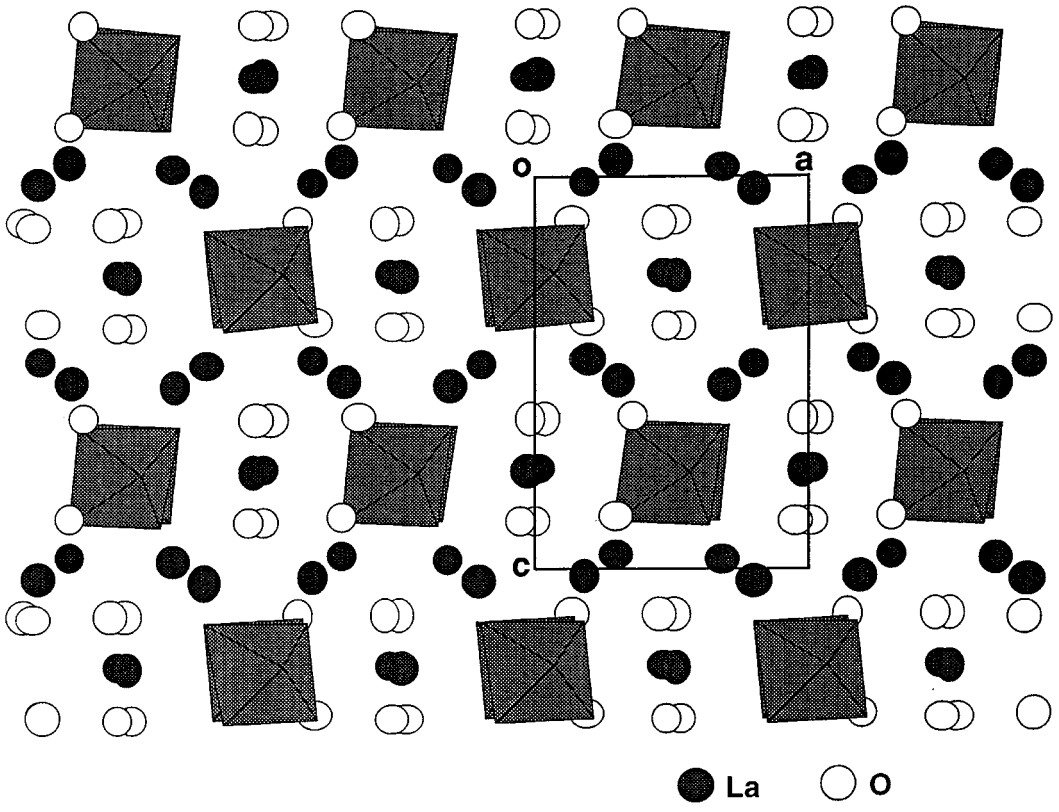

FIG. 1. Projection of the structure of La_3MoO_7 in the *ac* plane. The MoO_5^{5-} octahedra are shaded.

contains only Mo^{5+} cations. The La(1) cation has seven oxygen atoms as its nearest neighbors at distances ranging between 2.419 (4) and 2.776 (4) Å and an eighth at 3.293 (5) Å which form a highly distorted cube (Fig. 3a). In La_3NbO_7, the La(1) O_8 pseudo-cube is more regular (2.433 (8) ($\times 2$), 2.443 (8) ($\times 2$), 2.642 (8) ($\times 2$), and 2.989 ($\times 2$) Å). The distortion observed in La_3MoO_7 results principally from a slight rotation of the MoO_6 octahedra around the helicoidal axis parallel to the *b*-axis which induces a splitting of the two longest La–O distances. Thus the two equivalent La–O distances of 2.988 Å in La_3NbO_7, give rise to the La(1)–O(5) and La(1)–O(3) distances of 2.776 (4) and 3.293 (5) Å, respectively, and those of 2.642 (8) Å to La(1)–O(2) and La(1)–O(4) of 2.494 (4) and 2.710 (4) Å in La_3MoO_7. The lanthanum ions which ensure the cohesion between the slabs occupy two crystallographically independent positions, La(2) and La(3). The La(2) and La(3) cations are both surrounded by seven oxygen atoms forming highly distorted pentagonal bipyramids (Figs. 3b and 3c). The La(2)–O distances range from 2.333 (3) to 2.669 (3) Å for the La(2) site and from 2.325 (3) to 2.614 (3) Å for the La(3) site, typical of values found for a sevenfold coordinate La cation. The mean La–O distances are 2.497 and 2.481 Å for these two sites, respectively. In La_3NbO_7, the La–O distances in the unique sevenfold coordinate La site are quite comparable with La–O distances lying between 2.341 (4) and 2.708 (2) Å and the mean value of 2.487 Å.

Crystal Structure 298–10 K

The room temperature crystal structure of La_3MoO_7 was described in the preceding section. Any changes in structure can be monitored most conveniently using powder neutron diffraction. Diffraction patterns were recorded at several temperatures between 200 and 10 K. No significant change in structure could be detected either by visual inspection of the patterns or from the details of the Rietveld fits. Also there was no evidence for any second phase in the bulk powder samples used for the susceptibility and magnetic neutron diffraction studies.

Resistivity

The temperature dependence of the electrical resistivity measured along the *b*-axis (direction of the chain of corner-linked MoO_6 octahedra) (Fig. 4) shows that La_3MoO_7 is semiconducting in the temperature range 144–300 K. The resistance below 144 K is greater than

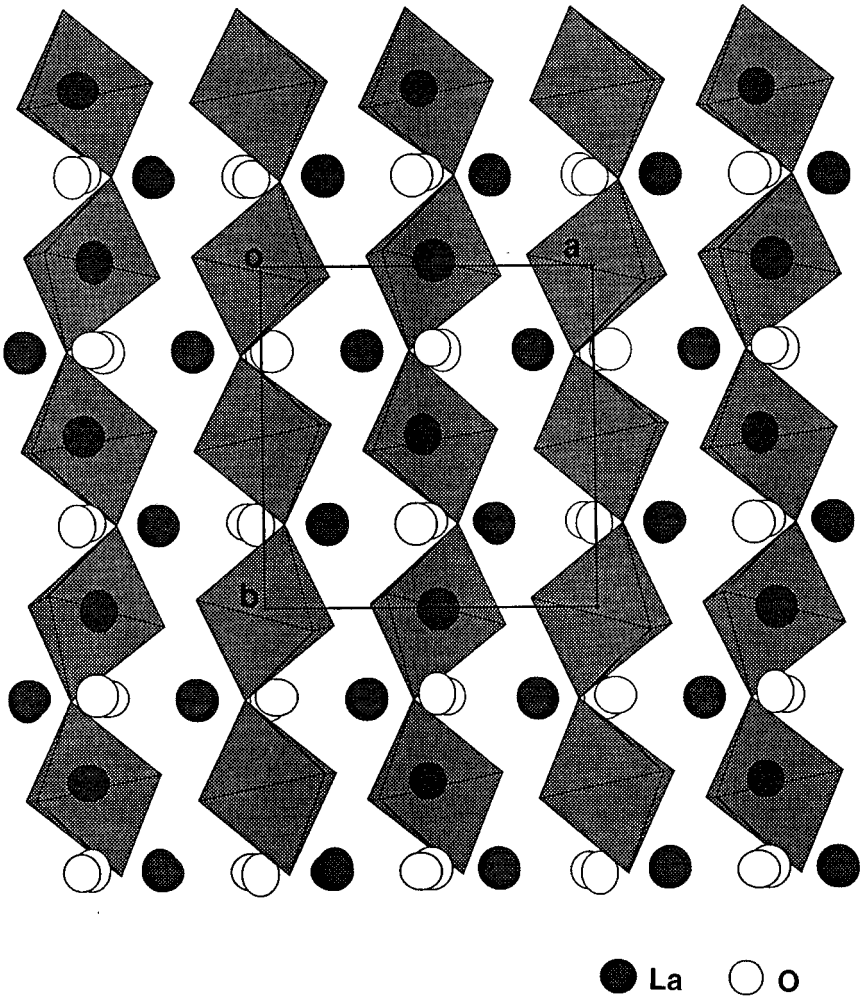

FIG. 2. Projection of the structure of La_3MoO_7 in the *ab* plane showing the corner sharing octahedral chains along *b*.

2 MΩ which is beyond the detection limit of our instrumentation. The room temperature resistivity is 11 ohm-cm and the activation energy calculated in the region 170–300 K (see inset) is 0.16 eV.

Magnetic Susceptibility

The results of the susceptibility measurements are shown in Fig. 5. Complex behavior is clearly indicated. The magnitude of the susceptibility is smaller than expected by about a factor of 10^{-2} for a simple $S = 1/2$ paramagnet. First, note that even up to 800 K there is no Curie–Weiss regime and apart from the region below 100 K, the susceptibility increases with increasing temperature up to a broad maximum at about 655 K. In view of the presence of the MoO_5 chains, it is tempting to assign this maximum to one-dimensional short-range magnetic correlations. To provide convincing evidence for this would require fitting data well above the maximum and such data do not, unfortunately, exist. Continuing with this assumption an intrachain J/k can be estimated from the relationship for a $S = 1/2$ one-dimensional Heisenberg model,

$$k\chi(T_{max})/J = 1.282,$$

which yields $J/k = -511$ K.

Apart from the broad maximum there appear to be at least three other notable features in the data of Fig. 5, namely a kink at about 483 K, a sharp decrease below 140 K, and an increasing susceptibility below 100 K. The feature at 483 K may indicate a phase transition which is perhaps crystallographic in origin. DSC evidence, Fig. 6, supports the presence of a phase transition in the form of

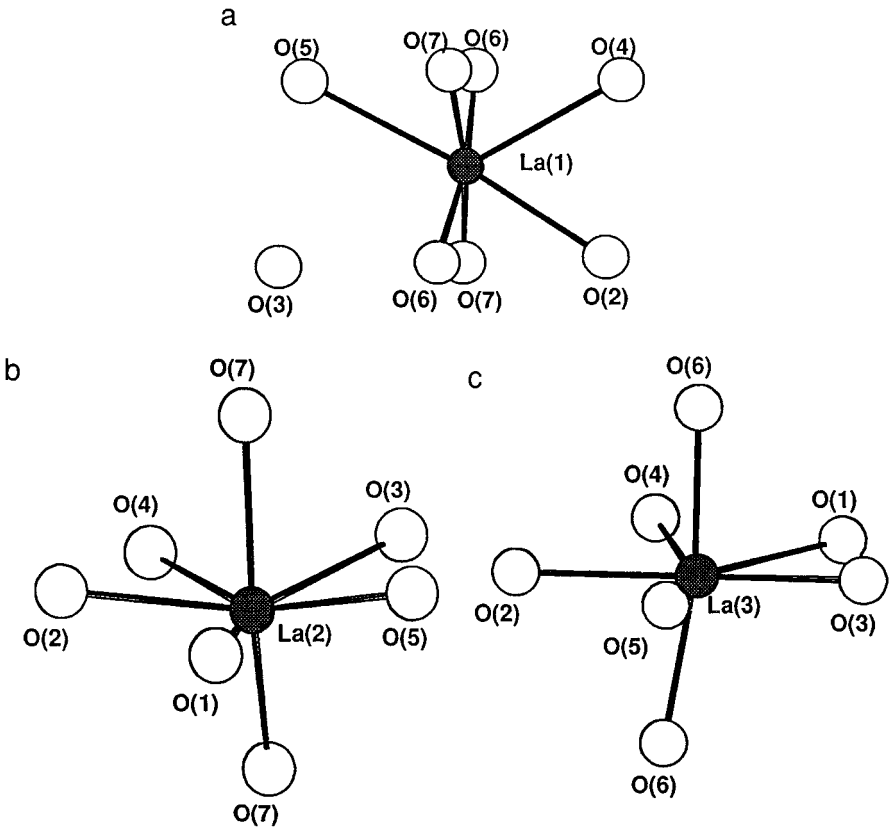

FIG. 3. The coordination polyhedra around La (1) (a), La (2) (b), and La (3) (c).

a relatively sharp peak at 481 K. Note also evidence for another transition at lower temperature, 373 K, which is not apparently reflected in the susceptibility. The decrease in χ below 140 K may indicate the onset of interchain coupling and the increase below 100 K may be associated with a paramagnetic impurity or could also signal a weak spontaneous moment due to a spin canted, long-range ordered antiferromagnetic structure. For a noncentrosymmetric space group such as $P2_12_12_1$, a spin canted structure would be expected.

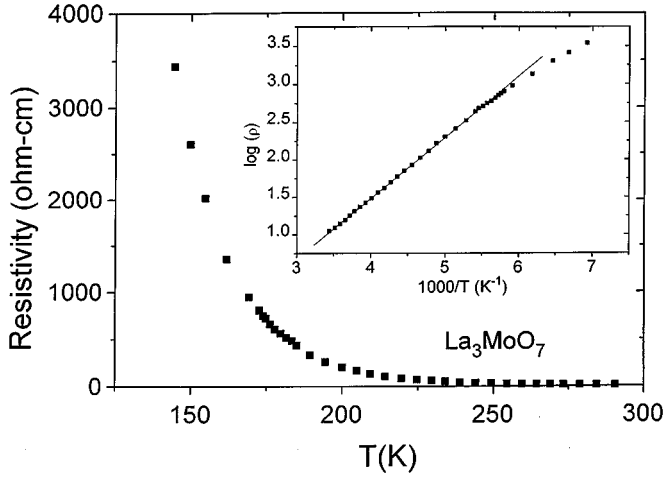

FIG. 4. Resistivity for a La_3MoO_7 crystal measured along the *b*-axis. The inset shows a single activation energy in the range 170–300 K.

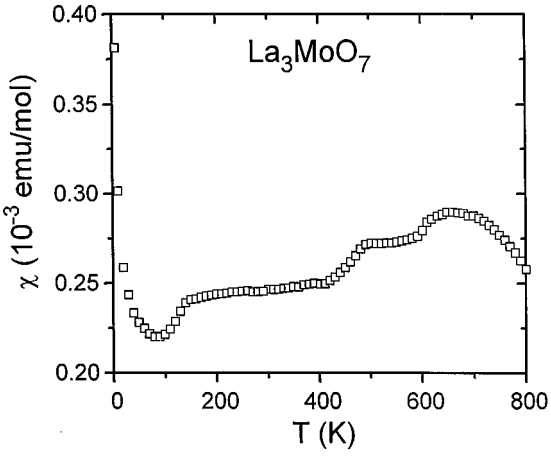

FIG. 5. Magnetic susceptibility data for La_3MoO_7. The measuring field is 100 Oe.

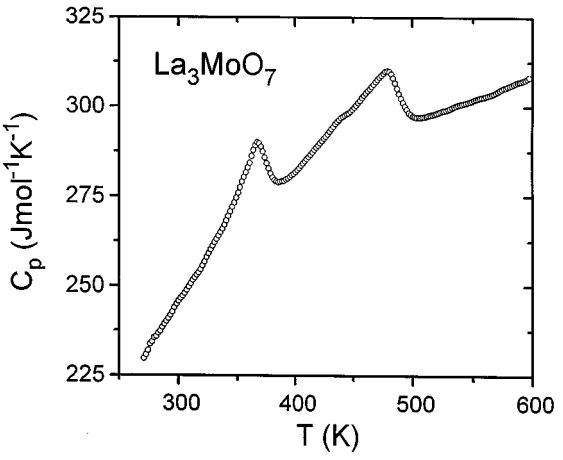

FIG. 6. Specific heat data for La_3MoO_7 above room temperature.

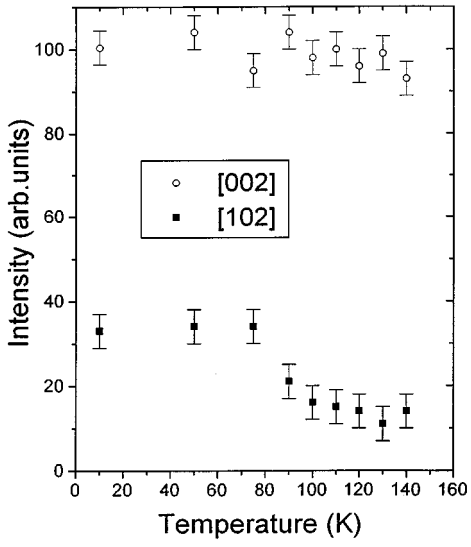

FIG. 7. Temperature dependence of the (002) and (012) reflections as a function of temperature for La_3MoO_7.

This hypothesis was investigated by neutron diffraction experiments in the temperature range 10 to 160 K. Visual inspection of the data sets showed that one weak reflection, the (102), had a marked temperature dependence consistent with ordering near 100 K. This is shown in Fig. 7 along with the nonmagnetic (002) for comparison. Figures 8a and 8b display the portion of the powder pattern containing this reflection at 10 K. In Fig. 8a the solid line is a fit to the structural model only, while in Fig. 8b a magnetic structure is included in which the spins within each chain are coupled antiparallel and also antiparallel to nearest neighbors in adjacent chains. A magnetic moment of $0.87(2)\,\mu_B$ per Mo(5+) is refined which is consistent with a $S = 1/2$ ion. The $R_{mag} = 0.17$ is satisfactory given the weakness of the intensities involved. For this model there is a significant magnetic component only for the (111) and (012) reflections. Although the evidence just cited for long-range magnetic order below 100 K is reasonably sound, no explanation for the 140 K anomaly is available from the neutron data.

Finally, it should be noted that the susceptibility data for La_3MoO_7 reported here are very different from those presented previously (4), in which Curie–Weiss behavior was found over the temperature range 100–250 K. The susceptibility values of (4) are higher at all temperatures than those

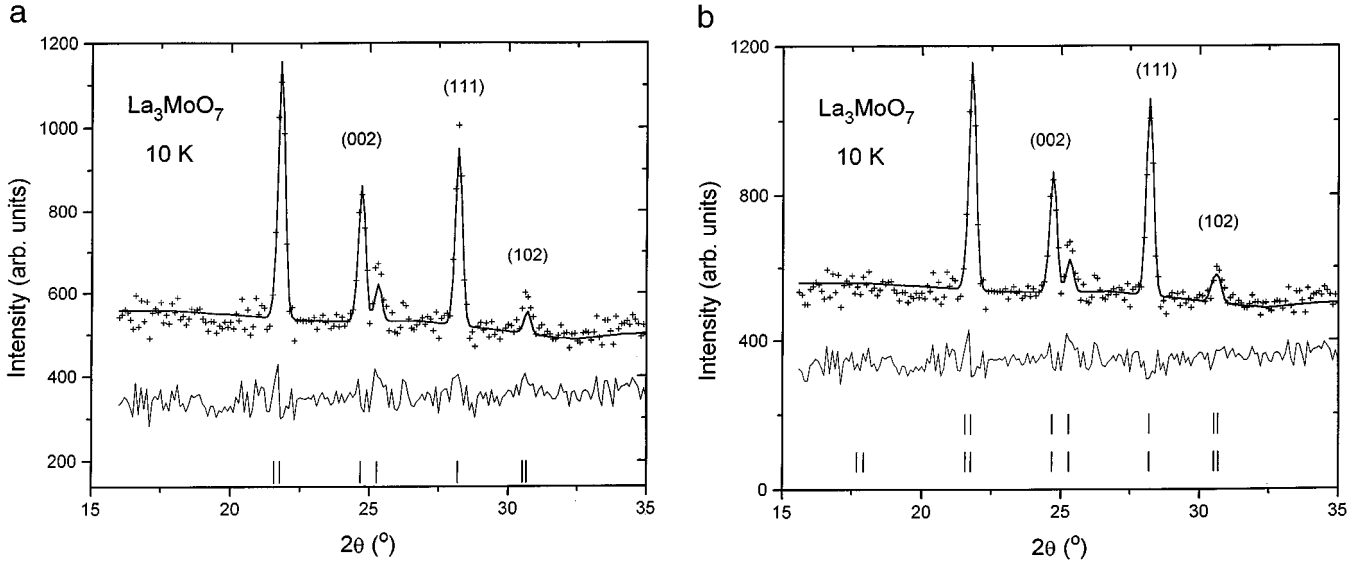

FIG. 8. (a) Low angle neutron diffraction patterns at 10 K for La_3MoO_7. The solid line is a fit to the structural model only. Note the poor fits at (111) and (012). (b) The same data as in 8a but this fit includes a magnetic structure model described in the text. The fits at (111) and (012) are much improved.

of Fig. 5, by factors of two near 250 K increasing to factors of five to ten below 50 K. A detailed explanation for these differences is not clear but two points can be made. First, the authors of (4) indicate that their sample contains impurities, "a large amount" of albeit diamagnetic impurities, but the phases are not identified. Secondly, there is a small difference in the unit cell volumes, 649 $Å^3$ in (4) and 651 $Å^3$ here. In any case the results reported in the present work are consistent with the one-dimensional character of the MoO_5^{5-} chains in the structure.

SUMMARY

The crystal structure of La_3MoO_7 has been solved in $P2_12_12_1$, a space group not previously found for materials of the Ln_3MO_7 type. The key feature of the structure is the presence of chains of *trans*-corner-shared octahedra, MoO^{5-}, parallel to the *b*-axis. The Mo–O–Mo angle is 149° and the Mo–Mo distance is uniform within the chain. This precludes the presence of Peierls distortion. Single crystal resistivity data taken parallel to the *b*-axis show semiconducting behavior from 298 to 140 K with a fairly large activation energy of 0.16 eV. This indicates that the *d* electrons are localized in La_3MoO_7. Magnetic susceptibility data are consistent with a strong intrachain antiferromagnetic coupling with a $J/k = -511$ K. There are several other anomalies in the susceptibility and heat capacity. One at 483 K is present in both the susceptibility and heat capacity and may be due to a structural transformation but one at 373 K is not seen in the susceptibility. A sharp susceptibility decrease sets in below 140 K and then an increase is seen below 100 K. There is neutron diffraction evidence for long-range antiferromagnetic ordering below 100 K but the 140 K anomaly is unexplained. The local moment magnetism of La_3MoO_7 is unusual for molybdenum oxides. The one-dimensional character and the very acute Mo–O–Mo angle may be key factors in the localization mechanism.

ACKNOWLEDGMENTS

We acknowledge support of the research performed at McMaster by the Natural Science and Engineering Research Council of Canada. We thank C. V. Stager for use of the SQUID magnetometer, R. Donaberger and I. Swainson of AECL for assistance with the neutron diffraction experiments, and H. G. Gibbs for the DSC data.

REFERENCES

1. H. P. Rooksby and E. A. D. White, *J. Am. Ceram. Soc.* **47,** 94 (1964).
2. J. G. Allpress and H. J. Rossell, *J. Solid State Chem.* **27,** 105 (1979).
3. H. J. Rossell, *J. Solid State Chem.* **27,** 115 (1979).
4. H. Prevost-Czeskleba, *J. Less-Common Met.* **127,** 117 (1987).
5. W. A. Groen, F. P. F. van Berkel, and D. J. W. IJdo, *Acta. Crystallogr. C* **43,** 2262 (1987).
6. J. F. Vente and D. J. W. IJdo, *Matter. Res. Bull.* **26,** 1255 (1991).
7. J. F. Vente, R. B. Helmholdt, and D. J. W. IJdo, *J. Solid State Chem.* **108,** 18 (1994).
8. A. Kahn-Harari, L. Mazerolles, D. Michel, and F. Robert, *J. Solid State Chem.* **116,** 103 (1995).
9. G. Wltschek, H. Paulus, I. Svoboda, H. Ehrenberg, and H. Fuess, *J. Solid State Chem.* **125,** 1 (1996).
10. A. C. T. North, D. C. Phillips, and F. S. Mathews, *Acta. Crystallogr. A* **24,** 351 (1968).
11. H. D. Flack, *Acta. Crystallogr. A* **39,** 876 (1983).
12. G. M. Sheldrick, "SHELXL93, Program for the refinement of Crystal Structures." Univ. of Gottingen, Germany.
13. Enraf-Nonius, "CAD-4 Software. Version 5.0." Enraf-Nonius, Delft, The Netherlands, 1989; K. Fair, "MOLEN User's Manual. An interactive Intelligent System for Crystal Structure Analysis." Enraf-Nonius, Delft, The Netherlands.
14. R. D. Shannon, *Acta. Crystallogr. A* **32,** 751 (1976).
15. J. Tortelier and P. Gougeon, *Acta. Crystallogr. C* **52,** 500 (1996).